Cerebral Cortex Advance Access published September 12, 2014
Cerebral Cortex
doi:10.1093/cercor/bhu199

The Default Mode Network Differentiates Biological From Non-Biological Motion

Eran Dayan[1,2,5,†], Irit Sella[2,†], Albert Mukovskiy[3,4], Yehonatan Douek[1], Martin A. Giese[3,4], Rafael Malach[2] and Tamar Flash[1]

[1]Department of Computer Science and Applied Mathematics, [2]Department of Neurobiology, Weizmann Institute of Science, Rehovot 76100, Israel, [3]Department of Cognitive Neurology, Hertie Institute for Clinical Brain Research, Tübingen, Germany and [4]Center for Integrative Neuroscience, University Clinic Tübingen, Tübingen 72076, Germany

[5]Present Address: Human Cortical Physiology Section, National Institute of Neurological Disorders and Stroke, National Institutes of Health, Bethesda, MD 20892 USA

Address correspondence to Email: dayane@ninds.nih.gov (E.D.); tamar.flash@weizmann.ac.il (T.F.)
[†]Eran Dayan and Irit Sella contributed equally to this work.

The default mode network (DMN) has been implicated in an array of social-cognitive functions, including self-referential processing, theory of mind, and mentalizing. Yet, the properties of the external stimuli that elicit DMN activity in relation to these domains remain unknown. Previous studies suggested that motion kinematics is utilized by the brain for social-cognitive processing. Here, we used functional MRI to examine whether the DMN is sensitive to parametric manipulations of observed motion kinematics. Preferential responses within core DMN structures differentiating non-biological from biological kinematics were observed for the motion of a realistically looking, human-like avatar, but not for an abstract object devoid of human form. Differences in connectivity patterns during the observation of biological versus non-biological kinematics were additionally observed. Finally, the results additionally suggest that the DMN is coupled more strongly with key nodes in the action observation network, namely the STS and the SMA, when the observed motion depicts human rather than abstract form. These findings are the first to implicate the DMN in the perception of biological motion. They may reflect the type of information used by the DMN in social-cognitive processing.

Keywords: action-perception coupling, biological motion, default mode network

Introduction

Despite years of continued interest, the functional role of the default mode network (DMN) remains a topic of debate (Buckner et al. 2008; Anticevic et al. 2012; Mantini and Vanduffel 2013). The DMN is composed of distinct brain regions along medial prefrontal, medial and lateral parietal, and medial and lateral temporal cortices, which are consistently more active during rest periods and are deactivated when subjects are engaged in externally oriented cognitively demanding tasks (Raichle et al. 2001; Buckner et al. 2008). Abundant evidence points toward the involvement of the DMN in various social-cognition functions (Corbetta et al. 2008; Mars et al. 2012), including self-referential processing (Buckner et al. 2008; Qin and Northoff 2011; Whitfield-Gabrieli et al. 2011; Mantini and Vanduffel 2013), mentalizing, and theory of mind (Mars et al. 2012). More specifically, frontal structures along the midline as well as other parts of the DMN have been implicated in an array of high-level self-related functions, including self-projection (Buckner and Carroll 2007), encoding and retrieval of autobiographical memories (Spreng et al. 2009), and self-evaluation (Gusnard et al. 2001). Similarly, core DMN regions have been linked with functions related to theory of mind such as mental state attribution (Saxe and Powell 2006) and perspective taking (Ruby and Decety 2001). Yet, the properties of external and internal stimulation that elicit activity within the DMN in relation to these social-cognitive functions remain unknown.

A powerful source of information utilized by the brain for self-referential processing and theory of mind-related computations is motion kinematics (Pavlova 2012). For example, self and other-generated actions can be distinguished based solely on the observed motion kinematics (Knoblich and Prinz 2001; Daprati et al. 2007). Motion kinematics was also shown to underlie functions such as intention understanding (Becchio et al. 2008, 2012) and mentalizing (Frith and Frith 2006). In addition, atypical kinematics has been observed in movement production by individuals with autism spectrum disorder (Cook et al. 2013), a disorder that carries known deficits in mentalizing and theory of mind. Thus, altogether, converging lines of evidence imply that activity within the DMN might be tuned to the temporal and spatial features of movement as captured by movement kinematics. However, to date, this hypothesis has not been examined, since prior attempts to map the functionality of the DMN have focused on high-level cognitive and social functions.

Here, we set up to examine whether the DMN, localized functionally, differentiates between biological (natural) and non-biological motion kinematics. Based on our previously published paradigm (Dayan et al. 2007; Casile et al. 2010), we parametrically manipulated the motion of a human-like avatar and of an abstract object devoid of human-like form to either comply with or violate the so-called two-thirds power law (see Materials and Methods), a ubiquitous feature of motion production that describes the relationship between the speed and geometric curvature of curved movements (Lacquaniti et al. 1983). Thus, the stimuli depicted motion with biological versus non-biological kinematics, having human-like form, or more abstract form-features. Analyses then focused on the effects these manipulations of motion kinematics have on DMN activity and connectivity.

Materials and Methods

Participants

Eighteen subjects (11 females, mean age 28 years ± 4 SDs) were recruited for this study. All subjects were right-handed and had normal or corrected-to-normal vision. Participants gave their written informed consent. The Tel Aviv Sourasky Medical Center Institutional Review Board approved all experimental procedures. The data from 3 subjects were excluded due to excessive head motion ($n = 2$) or technical

problems during data acquisition ($n = 1$); therefore, our final sample of subjects comprised 15 participants.

Task and Stimuli

Motion Stimuli

The two-thirds power law is an empirically derived expression describing the strong relation that exists between the kinematics of motion and the geometrical features of the path followed by the hand during planar drawing movements. In the special case of drawing movements, the geometry–kinematics relation can be described with the following expression:

$$A = KC^{\beta} \quad (1)$$

where A and C denote angular velocity and path curvature, respectively, and K is the velocity gain factor, which is piecewise constant during entire movement segments. It has been shown that for ellipses, the exponent β in Equation 1 is very close to 2/3; thus, this relationship has been referred to as the "two-thirds power law." In this study, we used an analogous expression to Equation 1 using tangential velocity, V, rather than angular velocity and using radius of curvature, R, rather than the path curvature:

$$V = KR^{\beta} \quad (2)$$

An exponent of $\beta = 1/3$ gives the 2/3 power law.

Motion stimuli were comprised of short video clips showing hand and arm movements of an avatar, based on the motions of a human actor recorded with a Vicon motion capture system (Vicon Motion Systems Ltd) using 7 cameras. Full-body motion data were captured with a temporal sampling rate of 120 Hz, and a spatial error of <1 mm. All motion clips were based on a single smooth and curvilinear movement in which the actor moved both arms as if writing in midair the trigram "lll." The recorded trajectory was filtered in MATLAB (MathWorks) using a fourth-order Savitzky–Golay filter with a window of 15 frames.

Three types of motions were then derived from the original captured human motion, resulting in 3 trajectories with identical paths (the original path) and overall duration (3 s) but with different velocity profiles. The first trajectory was the original trajectory, which had *natural* kinematics. The power relation between the tangential velocity and the curvature of the hand markers of the original trajectory was estimated to be $\beta = 0.377$, in agreement with the two-thirds power law and with previous reports for this type of smooth and curvilinear motions (Viviani and Flash 1995; Kandel et al. 2000; Casile et al. 2010). Two motions with unnatural kinematics were created, *counter-natural* kinematics and *hyper-natural* kinematics, each violating the two-thirds power law differently. Counter-natural denotes that contradictory to natural kinematics, motion speed is higher during curved segments of the path whereas it is lower during straight segments of the path (Fig. 1*A*). Hyper-natural denotes that similarly to natural kinematics, slowing-down occurs during curved segments of the path whereas speeding-up occurs during straighter path segments, although excessively compared with the natural velocity profile. Trajectories of unnatural kinematics were constructed by locally time-warping the original trajectory to fit either counter-natural kinematics ($\beta = -0.46$) or hyper-natural kinematics ($\beta = 0.559$). Time-warping was done by local linear re-sampling of the trajectory (in windows comprising 5 data points from the 120 fps data), such that local slowing-down or speeding-up of the trajectory fitted the desired relation between curvature and tangential velocity. β-values were chosen based on a pilot study where observers were asked to rate the naturalness of the motions. Once the new end-point trajectories were established, changes in trajectories were propagated from the wrist to the remaining arm segment and body data points by applying the same time warping procedure to the trajectories of the other recorded markers on the actor's body. The same procedure was applied to drawing movements in the opposite direction (i.e., counter-clock-wise instead of clock-wise), resulting in 3 additional trajectories of similar paths performed with natural, hypo-natural, and hyper-natural kinematic characteristics. All 6 trajectories were uniformly rescaled in time such that each stimulus lasted 3 s and had mean velocity of 0.163° and 0.167° per second for the right and left hand motions, respectively.

To create human-motion clips, full-body motion data were imported into a commercial software (3D StudioMax 9, Autodesk) where they were used to animate a human-like avatar. The face of the avatar was masked with a gray ellipsoid in order to minimize non-related activations of cerebral structures involved in face processing. Finally, rendering was done at 30 fps, and 6 human-motion AVI files were produced. To create abstract-motion clips, only the moving hand trajectories were used, serving as the center of a randomly distributed cloud of dots. Six AVI files at 30 fps were created in MATLAB. Thus, human-motion and abstract-motion clips were identical with respect to their kinematics but differed with respect to the form of the moving agent/object.

Experimental Design

The experiment included 5 functional scans, 2 scans with human-motion stimuli, 2 scans with abstract-motion stimuli, and a DMN-localizer scan, acquired during a single session. The 4 motion scans were collected first, and their internal order was counter-balanced across subjects. Motion scans comprised 27 blocks of 9-s presentations of motion stimuli followed by either 6- or 9-s fixation periods, resulting in scans with duration of 7 min and 45 s. Each block comprised a continuous concatenation of 3 motion clips of the same kinematic type, i.e., 3 natural, 3 counter-natural, or 3 hyper-natural clips (Fig. 1). In order to maintain subjects' attention to the observed motions, they were asked to perform a one-back memory task concerning the direction of the motion and to press a button when observing 2 consecutive clips of motions in the same direction. In 67% of the blocks, the direction of motion alternated between 2 consecutive motion clips. The other 33% of the blocks were target blocks in which 2 consecutive motion clips were in the same direction, either the first and second or the second and third clips. Target blocks were evenly distributed among natural, counter-natural, and hyper-natural kinematics. The block order within a scan was randomized. A fixation mark was present in the middle of the screen such that it was visible at all times. The subjects were instructed to maintain their gaze on it throughout the scan.

The DMN was localized functionally (e.g., Fair et al. 2007) in a separate functional scan using a semantic sensory-motor task. Subjects were shown written nouns and were asked to press a button if the noun described an animate creature. Nouns included words such as "umbrella," "girl," and "germ" (presented in Hebrew). Nouns were presented in 20 blocks (3 consecutive nouns, each presented for 3 s), each lasting 9 s, which were separated by fixation periods of 6 s, resulting in a scan of duration of 5 min and 18 s. A short (six-noun) training session of this task was held prior to entering the magnet.

MRI Data Acquisition and Preprocessing

Subjects laid supine in the scanner and viewed a back-projected screen located above their heads through an angled mirror. Stimuli were delivered via the software Presentation (www.neurobs.com), which was synchronized with the MR pulses. Subjects' index and middle fingers were placed over a button in an MR compatible response box, and their responses were recorded for later behavioral analysis. Functional and anatomical images of the brain were acquired with a Siemens 3T Trio MRI scanner equipped with a birdcage head coil used to transmit and receive RF. Blood oxygenation level-dependent (BOLD) contrast was obtained using a T2*-sensitive gradient-echo echo-planar imaging (GE EPI) pulse sequence with a repetition time (TR) of 3000 ms, echo time (TE) of 30 ms, flip angle of 90°, 46 slices, $3 \times 3 \times 3$ mm voxels, and field of view of 216 mm. High-resolution anatomical volumes were acquired with a T1-weighted 3D-MPRAGE pulse sequence ($1 \times 1 \times 1$ mm).

MRI data were preprocessed and analyzed using Brain Voyager QX (Brain Innovation) and custom routines written in MATLAB (MathWorks). The first images of each functional scan were discarded to allow the scanner to reach steady-state magnetization. Functional scans were then subjected to slice scan-time correction, 3D motion correction, which involved re-sampling with trilinear interpolation, temporal

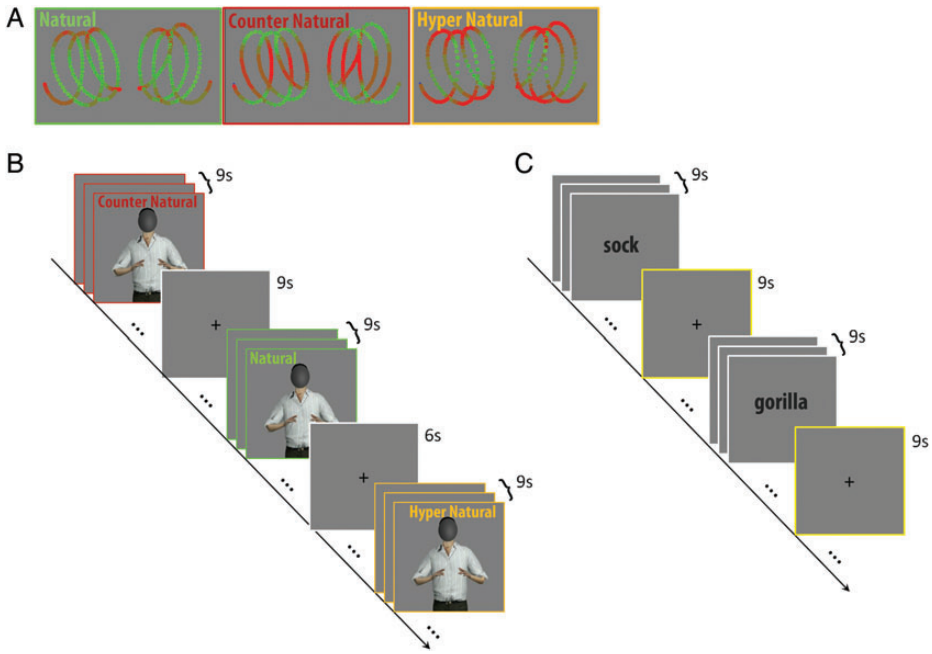

Figure 1. Task and stimuli. (*A*) Illustration of the 3 types of dependencies between speed and curvature used in the motion-observation task. In natural kinematics, the two-thirds power law is preserved, such that the curved segments of the path are traced with slower speed compared with straight segments. In counter-natural kinematics, the relation between curvature and speed is reversed. In hyper-natural kinematics, the relation between curvature and speed is exaggerated relative to natural motion with excessive slowing-down at curved segments. (*B*) Timeline for motion-observation task. Three sequential clips of an avatar performing bi-manual drawing movements were grouped according to their kinematic profile. Counter-natural and hyper-natural together comprised the unnatural condition. (*C*) Timeline for DMN localization task. Sequences of 3 nouns were presented for categorization as animate/non-animate.

high-pass filtering with a cutoff frequency of 3 cycles per scan, and Gaussian spatial smoothing with a kernel of 6-mm width. Functional images were aligned with the high-resolution anatomical volume using trilinear interpolation. Anatomical and functional images were then transformed to the Talairach coordinate system (Talairach and Tournoux 1988). The cortical surface from 1 subject was reconstructed from a high-resolution anatomical image. The procedure included gray and white matter segmentation, inflating the gray matter, cutting along several medial locations, including the calcarine sulcus, unfolding the cortical surface, and flattening of the resulting mesh. Inflated and flattened cortical maps were used for figure presentations, and activations on these maps were further smoothed for visualization purposes using a spatial filter with a kernel of 4-mm width.

Data Analysis

Initial statistical analysis was based on the general linear model (GLM) (Friston et al. 1995) and consisted of 2 levels of analysis. At the first level, the time series of each voxel for each subject and functional scan were fitted with a design matrix. For the motion scans, a regressor was fitted for each of the kinematic conditions (natural, counter-natural, and hyper-natural). Our main focus was on the contrast [natural > unnatural], where unnatural refers to the combined regressor of the 2 unnatural motion conditions [counterNatural + hyperNatural] and the contrast is balanced for unequal number of repetitions. The regressors were modeled as boxcar functions convolved with the canonical hemodynamic response function. For each regressor, the baseline was defined by setting the value of the associated weights to zero. At the second level, a random-effect GLM was applied to the individual parameter estimates obtained from the first-level analysis. Statistical maps of contrasts were corrected for multiple comparisons at $P < 0.05$ using a cluster-threshold estimation procedure based on a Monte-Carlo simulation.

DMN Localization and Region of Interest Analysis

To identify the DMN, we employed a single-subject independent component analysis (ICA) comprising 30 components on the BOLD responses of the semantic task, followed by a second-level group analysis based on Self-organizing group-level ICA (SogICA) (Esposito et al. 2005). The analysis revealed a single independent component (IC) in extensive agreement with previous reports on the DMN, whereby the center of mass of each of the regions of the IC fell within previously reported DMN sub-divisions (Greicius et al. 2003; Buckner et al. 2008) (Supplementary Table 1). Independent component analysis was preferred over the standard task-negative GLM approach to maximize correlated activity within spatially distributed regions, as expected from a network. Notwithstanding, the cortical distribution of the IC-DMN was very similar to the putative DMN localized by contrasting rest > task using the data from the same task (see Supplementary Fig. 1). Fourier spectral analysis of the single-subject component verified that over 88 ± 2.6% (std) of its content comprised frequencies of <0.1 Hz, well within the range of frequencies common for intrinsic connectivity within large-scale functional brain networks (Greicius et al. 2007) (Supplementary Fig. 1). Following the identification of DMN-ROIs, mean β-values of natural and unnatural motions were extracted for each participant, and two-tailed paired *t*-tests were conducted using Statistica software (StatSoft, Inc.) setting the significance level P at 0.0083 (adjusted for multiple comparisons using Bonferroni correction)

Connectivity Analysis

In order to assess within network connectivity, a weighted connectivity matrix was generated for each subject by calculating partial Pearson correlations between averaged time series of every pair of regions (nodes) in the network while controlling for signal arising from white matter regions and from CSF. Three connectivity matrices were computed for each subject using the time course of the semantic task that was used to localize the DMN, based on trials of observation of natural motion, and unnatural motion. Connectivity was visualized in part using BrainNet Viewer (http://www.nitrc.or/projects/bnv/). Similarity between 2 full connectivity matrices R and S was assessed by calculating RV coefficients (Robert and Escoufier 1976; Shinkareva et al. 2010):

$$\mathrm{RV}(R, S) = \frac{\mathrm{trace}(R^{\mathrm{T}} \times S)}{\sqrt{\mathrm{trace}(R^{\mathrm{T}} \times R) \times \mathrm{trace}(S^{\mathrm{T}} \times S)}} \quad (3)$$

A direct assessment of the difference in connectivity between observation of natural- versus unnatural-motion is problematic, since it is difficult to assess whether a single similarity score is high or low (Josse et al. 2008). We therefore chose to use the third connectivity matrix as a common reference matrix—the typical DMN-connectivity matrix. Thus, 2 RV-coefficient scores were calculated per subject: RV(DMN, nat) and RV(DMN, unnat). A pairwise Wilcoxon test was used to assess the differences between the 2 scores across subjects using Statistica (Statsoft, Inc.)

Additionally, a nodal-strength vector was derived from each connectivity matrix. This vector was constructed as the nodal sum of all connected weights (using The Brain Connectivity Toolbox (Rubinov and Sporns 2010)). As positive and negative correlations may reflect different types of neural connections, this analysis was conducted separately for the positive and for negative correlation values to avoid cancelation of positive and negative correlations by summation (Rubinov and Sporns 2011; Cole et al. 2012). However, as the negative correlations were a negligible portion of the network (positive DMN: 96.1 ± 5.6%; positive natural: 85.6 ± 13.9%; positive unnatural: 88.5 ± 11.9% of edges in the network), we report only results based on the positive correlations within the networks. The nodal summation of connected weights yielded vectors of 10 dimensions, with magnitude that represents the overall connectivity strength of the network and direction that represents the relative per-node network connectivity strength. A pairwise Wilcoxon test was conducted across subjects to assess the differences in overall network strength. To assess similarity in relative nodal-strength under different conditions, we employed cosine similarity. Cosine similarity between vectors x and y is the dot product of the normalized vectors; thus, it expresses the similarity in vectors' directions (see the following equation):

$$\cos\_\mathrm{sim}(x, y) = \frac{\mathrm{dot}(x, y)}{|x| * |y|} \quad (4)$$

As in the case of the full connectivity matrices, 2 nodal-strength-similarity scores were calculated per subject—one for the similarity in connectivity between DMN and natural motion (cos_sim(DMN, nat)), and the second one for the similarity in connectivity between DMN and unnatural motion (cos_sim(DMN, unnat). A two-tailed pairwise Wilcoxon test was then applied on the paired indices using Statistica software (Statsoft, Inc.).

Lastly, we assessed the interactions between the DMN and areas implicated in visual perception and observation of action. First, to localize early visual cortex, we chose clusters showing maximal activity in occipital cortex in the contrasts [human_natural + human_unnatural > rest] and [abstract_natural + abstract_unnatural > rest] (see Supplementary Table 2). Secondly, we focused on the action observation network (AON) (e.g., Cross et al. 2009). AON ROIs were defined based on a comprehensive meta-analysis focusing on neuroimaging studies of action observation (Caspers et al. 2010). AON ROIs were defined around the peak activations of 8 bilateral regions (Caspers et al. 2010; Supplementary Table 3). In order to ensure that AON ROIs contained only task-positive voxels, we excluded voxels for which the contrast [all-motions > baseline] resulted in deactivation. Interactions between the DMN and the AON were assessed by calculating the partial correlations between all pairs of nodes in the 2 networks, while controlling for signals arising from white matter regions and from CSF. Correlations were computed for each subject, in each motion condition—human-natural, human-unnatural, abstract-natural, and abstract-unnatural, and were then Fisher-z transformed. Analysis of network interactions between the DMN and the AON was computed by pooling together z values from all nodes in the 2 networks, to test for network-wide interactions, and also by pooling together bilateral AON nodes and testing their interactions with the DMN. A 2 × 2 repeated measures ANOVA was then conducted on the pooled z values, to assess whether connectivity was affected by the motion's form (human or abstract), its kinematics (natural or unnatural), or their interaction.

Results

To test whether the DMN differentiates biological from non-biological motion, based on movement kinematics, we asked subjects ($n = 15$) to observe the motion of a human-like avatar performing bi-manual drawing movements that either complied with or violated the two-thirds power law (Fig. 1*A*,*B*; see Materials and Methods for a mathematical formulation of the two-thirds power law). A second simple semantic categorization task (Fig. 1*C*) was used to functionally localize the DMN (Fair et al. 2007). Here, the subjects were asked to categorize visually presented nouns as either animate or non-animate. Although deactivation within the DMN is largely task-independent, we deliberately chose to localize typical DMN areas using a task fully unrelated to the perception of biological motion in order to minimize possible cross talk between the tasks.

We first assessed the degree of overlap among regions showing preferential BOLD responses to biological motion with the DMN. We thus first contrasted motion with natural and unnatural kinematics [natural > counterNatural + hyperNatural] recorded in the motion task (Fig. 1 and Materials and Methods; $P < 0.05$, cluster-level corrected for multiple comparisons). We found significantly higher BOLD activity for natural kinematics in medial prefrontal cortex (PFC), anterior and posterior cingulate gyri, supplementary motor cortex, bilateral parahippocampal gyri (PHG), bilateral middle temporal gyrus, and bilateral basal ganglia (Fig. 2 and Supplementary Table 4). Next, to independently localize the DMN in each of the subjects, we employed single-subject ICA (Himberg et al. 2004) of BOLD

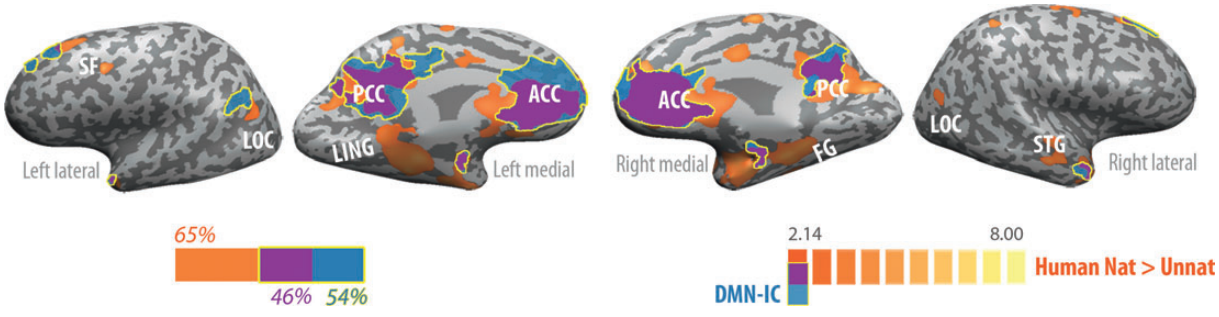

Figure 2. Preferential responses to natural versus unnatural motions (orange), DMN (blue), and regions of overlap (purple), on inflated cortices. Left bar depicts the proportion of voxels that were active in the motion task alone (orange), the DMN-IC alone (blue), and in both tasks (purple). Specifically, 46% of DMN voxels (blue and purple) also exhibited preferential activity to natural over unnatural human-motion observation (purple). ACC, anterior cingulate cortex; FG, fusiform gyrus; LING, lingual gyrus; LOC, lateral occipital cortex; PCC, posterior cingulate cortex; SF, superior frontal; STG, superior temporal gyrus.

responses for the semantic categorization task. Self-organizing group-level ICA (Esposito et al. 2005) revealed a single IC with a spatial layout in extensive agreement with previous reports on the DMN (Gusnard and Raichle 2001; Buckner et al. 2008). This single IC also overlapped with a standard task-negative univariate analysis, identifying areas that were deactivated by the semantic categorization task (see Materials and Methods and Supplementary Fig. 2). This overlap provided further support for classifying the single IC as being representative of the DMN. Notably, the DMN-IC revealed by this data-driven analysis overlapped with the set of regions that showed higher responses to natural motion (Fig. 2) along medial frontal and medial posterior, parietal, and temporal cortices. Specifically, 46% of the active voxels in the DMN showed preferential response to natural biological movements.

It should be noticed that the overlap between the 2 maps was restricted to regions where the preferential response to natural kinematics reflected a difference in the negative rather than the positive BOLD signals (Supplementary Fig. 3). In other words, observation of unnatural kinematics deactivated those regions more strongly compared with observation of natural kinematics.

To further examine the involvement of DMN regions in the differentiation of natural versus unnatural kinematics, we carried out a region of interest (ROI) analysis on the entire DMN-IC as well as on each of the 6 distinct bilateral regions that compose it. The DMN ROI definition was independent of the natural versus unnatural contrast. Unnatural kinematics deactivated the entire network significantly stronger compared with natural kinematics ($P < 0.005$, Fig. 3*B*). Specific regional analysis further revealed that deactivations were significantly stronger for unnatural compared with natural kinematics in 4 of 6 of the tested ROIs (Fig. 3*C*), including medial PFC and posterior cingulate, widely considered as the core areas of the DMN (Buckner et al. 2008), and also in bilateral middle temporal gyri and bilateral PHG ($P < 0.01$, Bonferroni-corrected for multiple comparisons). Of note, observation of the 2 types of kinematics that composed the unnatural condition (counter-natural and hyper-natural; see Materials and Methods) evoked statistically similar activity in all ROIs ($P > 0.05$ in all regions, except in the bilateral superior frontal gyri where the differences were significant, at $P > 0.01$, but did not pass the correction for multiple comparison). To confirm the specificity of these effects, we compared BOLD activity induced by natural and unnatural kinematics in a set of control ROIs, including right precentral, bilateral occipital, and bilateral superior parietal regions, all chosen based on their preferential responses to motion irrespective of kinematics (i.e., selected by contrasting natural + unnatural > rest). Task-induced activity in all control ROIs was similar for natural and unnatural kinematics ($P > 0.05$, Supplementary Fig. 4), indicating that the effects seen in DMN regions were not a general trend observed across functionally related and unrelated regions.

To further establish a link between the DMN and differentiation of unnatural from natural kinematics, we examined patterns of connectivity among DMN regions during the observation of these 2 types of motion. Nodes within the DMN were localized based on the IC analysis reported earlier (and were therefore identical to the previously reported ROIs; see Supplementary Table 1). We assessed connectivity differences within the DMN by generating a weighted connectivity matrix, calculated by correlating the time series of each pair of DMN nodes for each subject, separately for the natural and unnatural motion conditions, and for the semantic categorization task (Fig. 4*A*). We then reduced each connectivity matrix to a nodal-strength vector (Rubinov and Sporns 2010)—an ordered sum of the positive correlations of each node with all other nodes in the network (see Materials and Methods). Note that the magnitude of each nodal-connectivity vector represents the overall connectivity strength of the network whereas the direction of the vector represents the relative strengths of the nodes in the network. This analysis revealed no differences in DMN connectivity strength during the observation of unnatural and natural kinematics ($P = 0.324$).

More subtle differences in DMN connectivity during observation of natural versus unnatural kinematics were assessed by quantifying the degree of similarity these connectivity profiles display relative to that observed under the standard semantic categorization task design, assuming that the latter reflects the more typical non-motion-related DMN connectivity (Buckner et al. 2008; Andrews-Hanna et al. 2010). We thus calculated cosine similarity (Shinkareva et al. 2010; Braze et al. 2011) between each of the motion observation (natural and unnatural) nodal-connectivity vectors and the DMN-nodal-connectivity vector derived from the semantic categorization task (Fig. 4B). This resulted in 2 similarity indices per subject: cos_sim(DMN, nat) and cos_sim(DMN, unnat) (see Materials and Methods). This analysis revealed that cos_sim(DMN, unnat) was significantly larger than cos_sim(DMN, nat) (paired Wilcoxon, $P = 0.017$).

A secondary analysis was used in order to confirm these results, based on calculation of RV coefficients between the connectivity matrices (Robert and Escoufier 1976; Shinkareva et al. 2010). The RV coefficient is a multivariate extension of the Pearson correlation coefficient, which indicates the overall similarity of 2 matrices (Shinkareva et al. 2008, 2010; Piaggi et al. 2013). RV coefficients were calculated for each subject as a measure of the level of similarity between the DMN and observation of natural (RV(DMN, nat) and unnatural motion (RV(DMN, unnat). Note that RV is calculated on the full correlation matrices, which represent the complete and detailed connectivity profile of the networks, without dimension reduction or underlying assumptions. This analysis again revealed that similarity in connectivity was significantly larger for the unnatural compared with the natural motion (pairwise Wilcoxon, $P = 0.0076$; Fig. 4*C*).

It has been shown that for non-demanding tasks, the DMN is active during both rest and task periods (Greicius and Menon 2004). Therefore, for the main connectivity analyses, we chose to define typical DMN connectivity based on the entire time course of the semantic categorization task. Nonetheless, we repeated the connectivity analyses, defining the DMN based only on the fixation (rest) periods of the semantic categorization task. These analyses revealed a similar trend as the analyses conducted based on the full-time course. Full-matrix analysis revealed that (RV(DMN-fix, unnat) was significantly larger compared with RV(DMN-fix, nat) (pairwise Wilcoxon, $P = 0.01$). Similarity of nodal-strength also showed a non-significant trend similar to that reported above, whereby cos_sim(DMN-fix, unnat) was larger than cos_sim(DMN-fix, nat) (pairwise Wilcoxon, $P = 0.088$).

We next assessed the degree to which the observed differences in the neural responses to natural and unnatural kinematics may have reflected differences in the saliency associated with each of these types of motion and the attention

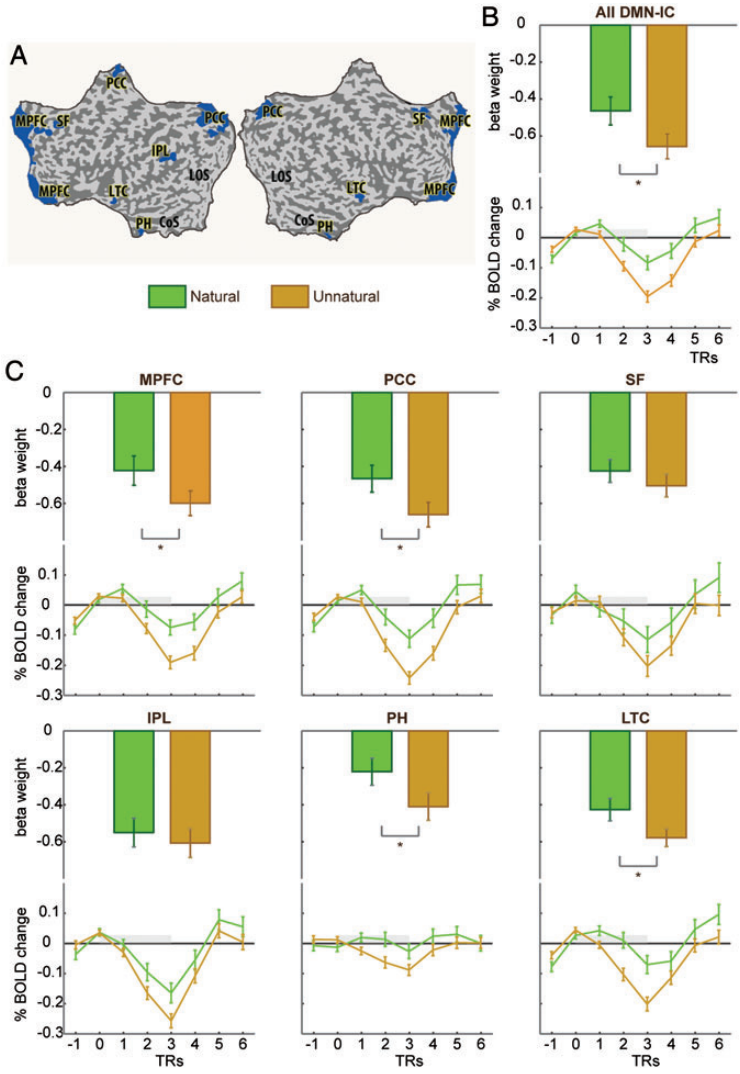

Figure 3. ROI analysis of natural versus unnatural motion in DMN-IC regions. Shown are β-values (top) and time courses (bottom) of BOLD responses to observation of natural (green) and unnatural (orange) kinematics. (*A*) ROIs are marked in blue on a flattened cortex. (*B*) The results for the entire DMN as an ROI. (*C*) The results for the 6 bilateral ROIs that compose the DMN-IC. Asterisks denote significant differences ($P < 0.05$ corrected for multiple comparisons). MPFC, medial prefrontal cortex; PCC, posterior cingulate and medial precuneus; SF, superior frontal gyrus; IPL, inferior parietal lobule; PH, parahippocampal gyrus; LTC, lateral temporal cortex.

allocated to them. The current experimental set-up required subjects to observe natural and unnatural kinematics while responding to a simple 1-back task, which was included in the design to keep subjects alert during the scans. The performance in this task (% successful detection of repeating stimuli) did not differ among the different motion conditions (paired Wilcoxon $P = 0.69$) suggesting that task difficulty and attention did not play a substantial role in the results reported here.

Variation in stimulus saliency and the associated differences in attention, which are reflected in stronger deactivation in the DMN, are typically also accompanied by higher positive BOLD signal in task-positive regions (McKiernan et al. 2003; Fox et al. 2005). In the current results, however, the stronger DMN deactivation in response to unnatural kinematics was not accompanied by stronger activation in task-positive regions. Whole-brain analysis did not reveal any regions where unnatural kinematics yielded stronger activity relative to natural kinematics. Subsequent ROI analysis focusing on regions that showed higher BOLD activity relative to baseline (unnatural > baseline) also failed to detect higher unnatural compared with natural activity ($P > 0.05$; Supplementary Fig. 5 and Supplementary Table 5). Additionally, 18 ROIs were localized at various frontal and parietal foci, in search for regions within the frontoparietal attentional network (Corbetta and Shulman 2002) (Supplementary Table 5) that could potentially reflect increased attention to unnatural compared with natural activity. Here, again, differences between the 2 motion conditions were not observed ($P > 0.05$; Supplementary Fig. 5). Altogether, these results imply that the differences in deactivation between natural and unnatural motion kinematics were not of an attentional origin.

We next examined whether the kinematic features of observed movement per se induce the specific responses observed here in DMN structures or whether motion-context also bares relevant information (Jastorff and Orban 2009). To that end, we assessed whether differential processing of

biological and non-biological kinematics exists within DMN structures when subjects viewed the motion of an abstract object (a cloud of dots) devoid of any human-like form features (Supplementary Fig. 6). Motion kinematics as well as task design in this experiment were otherwise identical to those of the human-form experiment. In accord with previous reports (Dayan et al. 2007), abstract natural motion evoked higher BOLD signals compared with abstract-unnatural primarily in primary and secondary visual areas in the occipital and temporal cortices as well as in the left inferior parietal, left postcentral gyrus, and left posterior cingulate. The difference between observed natural and unnatural abstract motion hardly overlapped with the DMN (2.5% DMN voxels also differentiated between abstract-natural and abstract-unnatural motions; Fig. 5, Supplementary Table 6). Nonetheless, we conducted ROI analysis with the same DMN-IC ROIs as in the human-form condition (Supplementary Table 1) to test for possible differentiation between natural- and unnatural-abstract motions. This test revealed only an insignificant trend for stronger deactivation in the unnatural condition (all P values > 0.07). We next repeated the connectivity analyses, as reported earlier, using the abstract-motion dataset. Consistent with the regional analysis, abstract-natural and abstract-unnatural were statistically indistinguishable with regards to their similarity with DMN connectivity, as recorded in the semantic categorization task (all P values > 0.4). Thus, these results suggest that although observation of natural and unnatural kinematics of an abstract object elicited markedly different brain responses, as reported before (Dayan et al. 2007), these 2 types of abstract motion did not differentially engage the DMN.

Lastly, to gain further insight into the involvement of the DMN in biological motion processing, we tested whether it interacts with other cortical regions implicated in visual perception and in perception of action and biological motion and

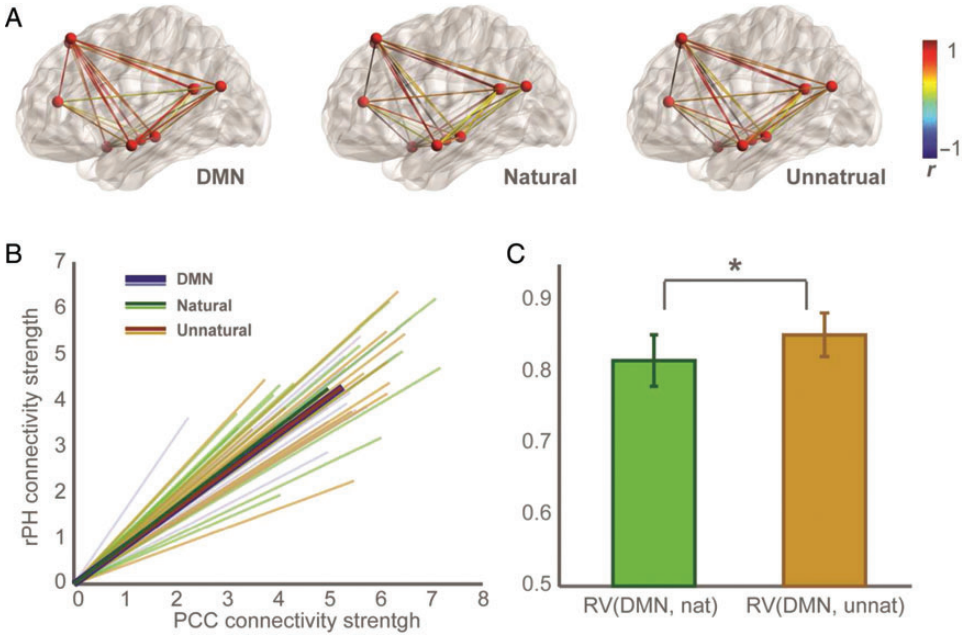

Figure 4. (*A*) Functional connectivity within areas comprising the DMN as recorded in the unrelated semantic categorization task (left) and during observation of natural (middle) and unnatural (right) motion. Data are from 1 representative subject. (*B*) Vectorial representation of nodal-connectivity strength on a reduced network (for illustration purposes). Vectors derived from single subjects' (thin lines) and averaged data (thick lines) are shown for each condition. Relative nodal connectivity (vector direction) was significantly more similar between DMN and unnatural, compared with natural kinematics. (*C*) RV coefficients indicating the degree of similarity between typical DMN connectivity and during observation of natural (RV(DMN, nat) and unnatural (RV(DMN, unnat) motion ($P < 0.00$).

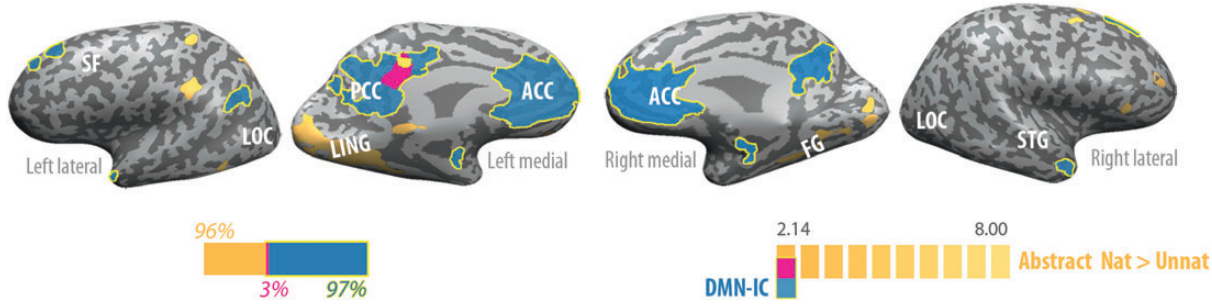

Figure 5. Preferential responses to natural versus unnatural abstract motion (yellow), DMN (blue), and regions of overlap (pink), on inflated cortices. Left bar depicts the proportion of voxels that were active in the motion task alone (orange), the DMN-IC alone (blue), and in both tasks (purple). Only 2.5% of DMN voxels, all in the ventral part of the left posterior cingulate, preferred natural over unnatural abstract motion. ACC, anterior cingulate cortex; FG, fusiform gyrus; LING, lingual gyrus; LOC, lateral occipital cortex; PCC, posterior cingulate cortex; SF, superior frontal; STG, superior temporal gyrus.

whether these interactions are modulated by the motion's kinematics and form. We first tested whether the DMN interacted with early visual cortex (see Materials and Methods and Supplementary Table 2). A 2 × 2 repeated measures ANOVA was conducted on the fisher's z-transformed correlation values, to assess whether DMN-early visual interactions were affected by the motion's form (human or abstract), its kinematics (natural or unnatural), or their interaction. This analysis revealed no significant effects (all P values > 0.08). We next focused on higher-order areas involved in the perception of action. Of particular interest is the so-called AON (e.g., Decety and Grezes 1999; Cross et al. 2009; Caspers et al. 2010), a distributed network of brain regions that preferentially respond to the observation of human action and motion. Nodes within the AON were defined based on a recent meta-analysis (Caspers et al. 2010) and encompassed bilateral frontal, parietal, temporal, and occipital regions (Fig. 6*A* and Supplementary Table 3). Interactions between the DMN and the AON were assessed on a network-wide and individual node basis for each subject and in each of the conditions (Fig. 6*B*). Analysis of network-wide interactions between the DMN and the AON, computed by pooling together all z values from each of the networks, did not reveal any significant effects (all P values > 0.1; Fig. 6*C*). On an individual bilateral AON node basis, a main effect for form was obtained for correlations between the DMN and the STS ($F_{1,14} = 7.06$, $P = 0.018$, Fig. 6*D*) and between the DMN and the SMA ($F_{1,14} = 6.61$, $P = 0.022$, Fig. 6*E*; for full results, see Supplementary Table 7). For both of these AON nodes, the coupling with the DMN was stronger when the stimuli had human rather than abstract form.

Discussion

The present study aimed to establish whether activity within the DMN differentiates biological from non-biological motion, based on compliance of motion with the characteristic kinematic features of human movement. Regions showing different task-induced deactivation in response to unnatural versus natural kinematics of a human-like avatar largely overlapped with the DMN, which was localized using an unrelated semantic categorization task. Detailed ROI analysis further revealed that unnatural human kinematics deactivated core DMN regions (4 of 6 regions in the network) more strongly than natural kinematics did. These differential effects were only

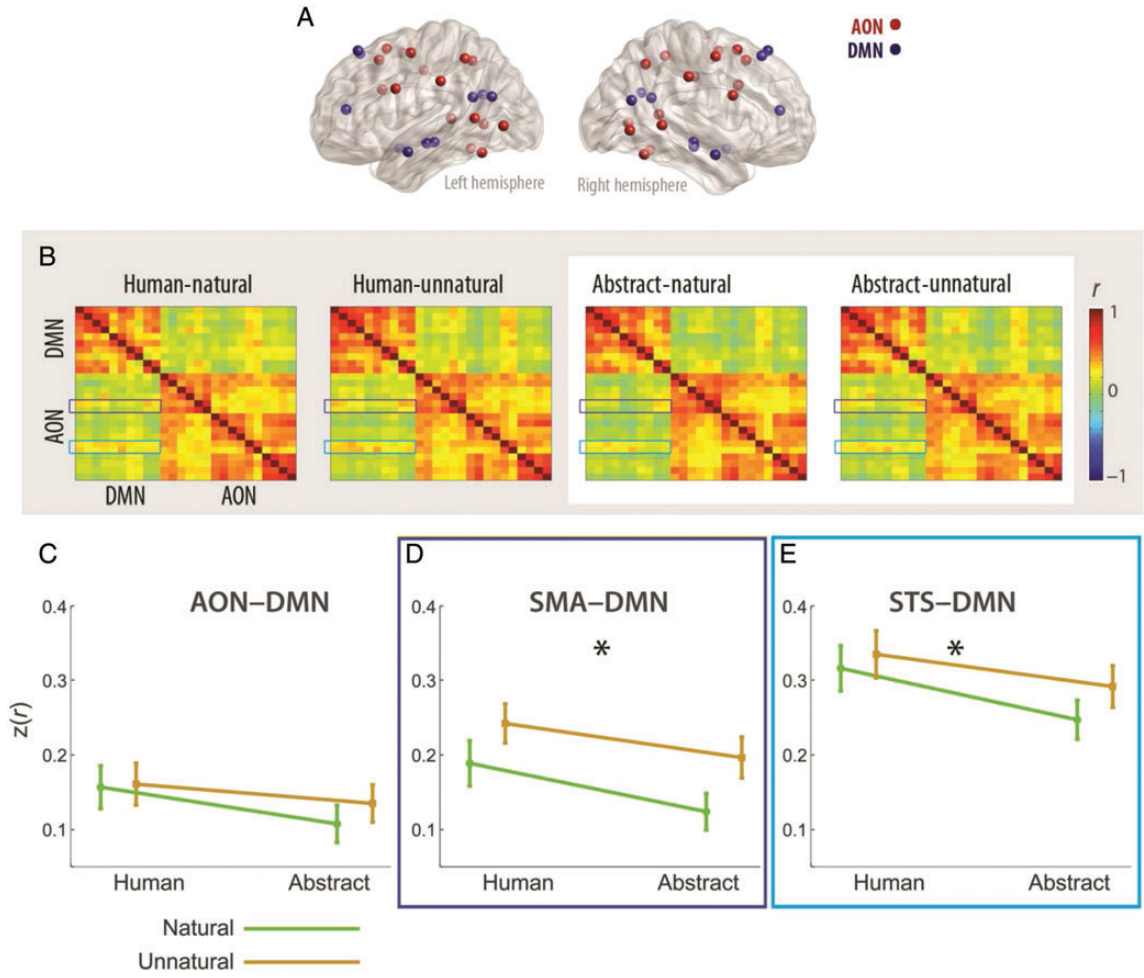

Figure 6. (*A*) Node locations for the DMN (as localized based on the IC analysis) and for the action observation network [AON, retrieved from (Caspers et al. 2010)]. (*B*) Connectivity matrices, expressing correlation strength between each pair of nodes in the DMN and the AON. Averaged matrices were generated for each condition (human-natural, human-unnatural, abstract-natural, abstract-unnatural). (*C*) 2 × 2 ANOVA revealed that network-wide connectivity between the DMN and the AON was not affected by the motion's form, kinematics, or their interaction. (*D*,*E*) In 2 AON nodes, the SMA (*D*) and the STS (*E*) connectivity with the DMN was stronger when the motion had human, relative to abstract form. *$P < 0.05$. All other effects were not significant (see Supplementary Table 7 for full results).

documented for the motion of a realistically looking human avatar and were not significant when the moving object was stripped from human-like form features. Connectivity within the DMN, as recorded in the unrelated semantic categorization task, resembled connectivity within the same regions more strongly during observation of unnatural rather than natural kinematics, further establishing that activity and connectivity within the DMN differentiate unnatural from natural kinematics. Finally, our data suggest that in differentiating between human and abstract form, the DMN is coupled more strongly with major nodes within the AON network, namely the STS and the SMA, when stimuli having human form are displayed. Overall, the results of this study suggest an undocumented role of the DMN in processing the characteristic kinematic features of observed human movement, thus differentiating between biological and non-biological motion of a human-like agent.

Despite continued interest (Anticevic et al. 2012), the functional role of the DMN is still a matter of debate (Gilbert et al. 2007; Golland et al. 2007; Buckner et al. 2008; Preminger et al. 2011; Anticevic et al. 2012). Thus, several interpretations of the results reported here can be offered. Cortical midline DMN structures, including medial PFC and anterior and posterior cingulate gyri, were consistently reported to be involved in various self-referential and other social-cognitive processes (Kelley et al. 2002; Mitchell et al. 2005; Goldberg et al. 2006; D'Argembeau et al. 2007; Qin and Northoff 2011; Mars et al. 2012), and the overlap between the DMN and regions implicated in social-cognitive functions has been noted and discussed before (Schneider et al. 2008; Qin and Northoff 2011; Whitfield-Gabrieli et al. 2011; Mars et al. 2012). The differential neural response to perceived motion complying with or defying natural kinematics observed here may reflect the processing of another basic aspect of social-cognitive processing within DMN structures, overlooked thus far—motion kinematics. It is possible that processing of human-like kinematics invokes stronger activation in cortical midline structures because it is within the motor capabilities of the observer, unlike unnatural kinematics, which is not (Viviani and Mounoud 1990). Indeed, earlier studies demonstrated that observation of action, which is within one's motor repertoire, activates medial PFC (Calvo-Merino et al. 2005). This pattern of activation could be reflected in smaller deactivation in response to natural compared with unnatural motion, as demonstrated here. Intermingled contribution to activation and deactivation within the DMN has been noted also in other experimental paradigms used in studies of social-cognitive processing, which often induce sensory- as well as internally-driven processes (Preminger et al. 2011). Our results also indicate that connectivity within DMN regions during observation of unnatural kinematics more closely resembled typical non-motion-related DMN connectivity compared with natural kinematics, possibly because only the latter contained self-like kinematic features that alter and perturb connectivity within this network. Interestingly, our results also indicate that differentiation of unnatural and natural kinematics in DMN structures required the moving object to have human-like form features, further suggesting that a degree of human resemblance or human context is required for DMN structures to differentiate biological from non-biological motion. It is possible that in human-relevant contexts, the DMN compares anticipated biological motion with actual observed motion, resulting in distinct activations when expectations are met (natural condition) versus when they are violated (unnatural condition). With no human-relevant context, expectations for biological motion cannot be established. In line with this suggestion, paracingulate regions have been recently associated with comparator functions of expected versus observed aspects of biological motion (Gowen and Poliakoff 2012).

Many studies have reported task-induced deactivation in DMN regions in response to cognitively demanding tasks (Raichle et al. 2001; Greicius et al. 2003; Fox et al. 2006), showing a relation between the magnitude of deactivation and externally oriented task difficulty or stimulus saliency (McKiernan et al. 2003; Gilbert et al. 2012). Despite a perceivable difference between the different motion stimuli used here (Levit-Binnun et al. 2006; Dayan et al. 2012), we found no evidence for differences in saliency between them. Differences in attentional response are expected to be evident in task-positive activity (Fox et al. 2005, 2009); however, our analyses did not find such differences favoring the unnatural condition (which deactivated the DMN more strongly) over the natural condition. With respect to task difficulty, the current experimental set-up required subjects to observe natural and unnatural kinematics while responding to a simple 1-back task, which was included in the design to keep subjects alert during the scans. The performance in this task did not differ among the different motion conditions. The current results are therefore unlikely to reflect task difficulty or stimulus saliency per se; instead, they may stem from visual and motor familiarity and expertise (Calvo-Merino et al. 2006; Casile and Giese 2006), which contribute to the ease with which socially relevant natural motion should be processed relative to unnatural motion.

The results further suggest that during motion observation, the DMN interacts in a selective manner with major nodes within the AON, namely the STS and the SMA. Widely known for its involvement in movement-related functions (Picard and Strick 2001), the SMA appears to also have a consistent role in action observation (Caspers et al. 2010; Mukamel et al. 2010). Similarly, numerous studies have established a critical role for the STS in perception of biological motion and action (e.g., Grossman et al. 2000; Blake and Shiffrar 2007). In the macaque, the STS encodes action-related visual information, which is projected to the parieto-frontal mirror circuit (Rizzolatti and Sinigaglia 2010) via the ventral premotor cortex (Nelissen et al. 2011). Thus, by interacting with the STS and the SMA, the DMN may indirectly access the major circuitry implicated in action observation. This suggestion fits well with the role of the DMN in social-cognitive functions (Mars et al. 2012), which in turn strongly relies on perception of action and biological motion (Pavlova 2012). Moreover, the interactions between the systems point to a possible role of the DMN, an associative network (Buckner et al. 2008), in action-observation expertise, by mediating the retrieval and integration of the motor and sensory representations of observed actions (Loula et al. 2005; Calvo-Merino et al. 2006; Cross et al. 2006).

Interestingly, rather than showing antagonistic interactions, our results demonstrate that the DMN is coupled with the STS and the SMA in differentiating between human and abstract form. The DMN shows antagonistic relationship with a few major large-scale brain networks, primarily the dorsal attention network (Spreng et al. 2010) and the task-positive fronto-parietal control network (Uddin et al. 2009). This relationship may feasibly reflect competition over control of shared computational resources (Anticevic et al. 2012). Still, it was also

established that for self-related cognitive processing, the DMN may also be coupled with the frontoparietal control network (Spreng et al. 2010). Our results add to this framework by demonstrating that rather than responding in an antagonist fashion, the DMN is coupled more strongly with key nodes in the AON when the observed motion depicts human rather than abstract form.

Perception of human movement necessitates elaborate timing representations for how velocity changes over time. An overarching feature in models of motor and perceptual timing (e.g., Ivry and Schlerf 2008; Merchant et al. 2013) is the reliance of timing mechanisms on distributed brain systems, including the DMN (Morillon et al. 2009; Lloyd 2012). It was recently suggested that the DMN is engaged in continuous tracking of stimuli duration at the temporal resolution of seconds, whereas areas in the motor system track events with shorter durations (Morillon et al. 2009). Adding to this framework, our findings document links between these 2 timing systems, more specifically between the DMN and the SMA, a major component in the motor timing network (Macar et al. 1999, 2004; Morillon et al. 2009). Human-motion perception and further differentiation of biological and non-biological motion requires both instantaneous, moment-by-moment tracking of motion kinematics and instantaneous timing and possibly also slower more integrative processing that takes the entire movement duration and form into account. Thus, an interaction between the 2 timing systems may be required for such elaborate perception and differentiation to take place.

The involvement of the DMN in the perception of human motion may additionally reflect the complex sources of information utilized by the brain for this perceptual task. A recent computational model hypothesized that distributed interconnected brain systems may influence movement timing and duration based on a mixture of several geometries, particularly Euclidian, equi-affine, and full affine geometries (Bennequin et al. 2009). Indeed, movements that comply with the two-thirds power law are a unique example for the ubiquity of non-Euclidean geometries in the human brain, as they are equivalent to movement at a constant equi-affine speed (Pollick and Sapiro 1997; Flash and Handzel 2007). The DMN appears to be a particularity suitable brain system to subserve motor and perceptual timing. Regions within the DMN are among the most densely connected regions in the human brain, both functionally and structurally (Greicius et al. 2003; van den Heuvel and Sporns 2011). Recent studies assessing anatomical connectivity using diffusion-weighted imaging identified several DMN regions that are not only highly connected with other cortical and subcortical structures but also are inter-connected among themselves, thus allowing links among different functional modules in the brain (van den Heuvel and Sporns 2011). Thus, the results reported here may reflect the contribution of the widely inter-connected components of the DMN to the complex computations required for motor and perceptual timing.

Conclusion

Activity and connectivity within core regions of the DMN encode the characteristic kinematic features of human movement, thus differentiating between observed biological and non-biological motion of human agents. These results may reflect the type of information used by the DMN in social-cognitive processing. They may further reflect the reliance of biological motion processing on distributed neural networks, allowing cross-modal links between perceptual and non-perceptual circuitries. Altogether, our study uncovers an unexpected sensitivity of the DMN, which is typically considered to be a high-order cognitive network, to subtle quantitative manipulations of observed human-motion kinematics.

Supplementary Material

Supplementary material can be found at: http://www.cercor.oxfordjournals.org/.

Funding

This work was supported by the EU Commission, 7th Framework Programme: EC-ICT-257695 Vere, EC FP7-ICT-249858 TANGO, and EC FP7-ICT-248311 AMARSi. T.F. is an incumbent of the Dr. Hymie Moross Professorial Chair. M.G. and A.M. were also supported by EU projects ABC (PEOPLE-2011-ITN PITN-GA-011-290011), HBP (FP7-ICT-2013-FET-F/ 604102), and KOROIBOT (FP7-ICT-2013-10/ 611909), and the DFG (GI 305/4-1 and KA 1258/15-1), and BMBF, FKZ: 01GQ1002A.

References

Andrews-Hanna JR, Reidler JS, Sepulcre J, Poulin R, Buckner RL. 2010. Functional-anatomic fractionation of the brain's default network. Neuron. 65(4):550–562.

Anticevic A, Cole MW, Murray JD, Corlett PR, Wang XJ, Krystal JH. 2012. The role of default network deactivation in cognition and disease. Trends Cogn Sci. 16(12):584–592.

Becchio C, Manera V, Sartori L, Cavallo A, Castiello U. 2012. Grasping intentions: from thought experiments to empirical evidence. Front Hum Neurosci. 6:117.

Becchio C, Sartori L, Bulgheroni M, Castiello U. 2008. Both your intention and mine are reflected in the kinematics of my reach-to-grasp movement. Cognition. 106(2):894–912.

Bennequin D, Fuchs R, Berthoz A, Flash T. 2009. Movement timing and invariance arise from several geometries. PLoS Comput Biol. 5(7):e1000426.

Blake R, Shiffrar M. 2007. Perception of human motion. Annu Rev Psychol. 58:47–73.

Braze D, Mencl WE, Tabor W, Pugh KR, Constable RT, Fulbright RK, Magnuson JS, Van Dyke JA, Shankweiler DP. 2011. Unification of sentence processing via ear and eye: an fMRI study. Cortex. 47(4):416–431.

Buckner RL, Andrews-Hanna JR, Schacter DL. 2008. The brain's default network: anatomy, function, and relevance to disease. Ann N Y Acad Sci. 1124:1–38.

Buckner RL, Carroll DC. 2007. Self-projection and the brain. Trends Cogn Sci. 11(2):49–57.

Calvo-Merino B, Glaser DE, Grezes J, Passingham RE, Haggard P. 2005. Action observation and acquired motor skills: an FMRI study with expert dancers. Cereb Cortex. 15(8):1243–1249.

Calvo-Merino B, Grezes J, Glaser DE, Passingham RE, Haggard P. 2006. Seeing or doing? Influence of visual and motor familiarity in action observation. Curr Biol. 16(19):1905–1910.

Casile A, Dayan E, Caggiano V, Hendler T, Flash T, Giese MA. 2010. Neuronal encoding of human kinematic invariants during action observation. Cereb Cortex. 20(7):1647–1655.

Casile A, Giese MA. 2006. Nonvisual motor training influences biological motion perception. Curr Biol. 16(1):69–74.

Caspers S, Zilles K, Laird AR, Eickhoff SB. 2010. ALE meta-analysis of action observation and imitation in the human brain. Neuroimage. 50(3):1148–1167.

Cole MW, Yarkoni T, Repovs G, Anticevic A, Braver TS. 2012. Global connectivity of prefrontal cortex predicts cognitive control and intelligence. J Neurosci. 32(26):8988–8999.

Cook JL, Blakemore SJ, Press C. 2013. Atypical basic movement kinematics in autism spectrum conditions. Brain. 136(Pt 9):2816–2824.
Corbetta M, Patel G, Shulman GL. 2008. The reorienting system of the human brain: from environment to theory of mind. Neuron. 58(3): 306–324.
Corbetta M, Shulman GL. 2002. Control of goal-directed and stimulus-driven attention in the brain. Nat Rev Neurosci. 3(3):201–215.
Cross ES, Hamilton AFdC, Grafton ST. 2006. Building a motor simulation de novo: observation of dance by dancers. Neuroimage. 31(3): 1257–1267.
Cross ES, Kraemer DJM, Hamilton AFdC, Kelley WM, Grafton ST. 2009. Sensitivity of the action observation network to physical and observational learning. Cerebral Cortex. 19(2):315–326.
Daprati E, Wriessnegger S, Lacquaniti F. 2007. Kinematic cues and recognition of self-generated actions. Exp Brain Res. 177(1):31–44.
D'Argembeau A, Ruby P, Collette F, Degueldre C, Balteau E, Luxen A, Maquet P, Salmon E. 2007. Distinct regions of the medial prefrontal cortex are associated with self-referential processing and perspective taking. J Cogn Neurosci. 19(6):935–944.
Dayan E, Casile A, Levit-Binnun N, Giese MA, Hendler T, Flash T. 2007. Neural representations of kinematic laws of motion: evidence for action-perception coupling. Proc Natl Acad Sci USA. 104(51): 20582–7.
Dayan E, Inzelberg R, Flash T. 2012. Altered perceptual sensitivity to kinematic invariants in Parkinson's disease. PLoS One. 7(2):e30369.
Decety J, Grezes J. 1999. Neural mechanisms subserving the perception of human actions. Trends Cogn Sci. 3(5):172–178.
Esposito F, Scarabino T, Hyvarinen A, Himberg J, Formisano E, Comani S, Tedeschi G, Goebel R, Seifritz E, Di Salle F. 2005. Independent component analysis of fMRI group studies by self-organizing clustering. Neuroimage. 25(1):193–205.
Fair DA, Schlaggar BL, Cohen AL, Miezin FM, Dosenbach NU, Wenger KK, Fox MD, Snyder AZ, Raichle ME, Petersen SE. 2007. A method for using blocked and event-related fMRI data to study "resting state" functional connectivity. Neuroimage. 35(1):396–405.
Flash T, Handzel AA. 2007. Affine differential geometry analysis of human arm movements. Biol Cybern. 96(6):577–601.
Fox MD, Corbetta M, Snyder AZ, Vincent JL, Raichle ME. 2006. Spontaneous neuronal activity distinguishes human dorsal and ventral attention systems. Proc Natl Acad Sci USA. 103(26):10046–10051.
Fox MD, Snyder AZ, Vincent JL, Corbetta M, Van Essen DC, Raichle ME. 2005. The human brain is intrinsically organized into dynamic, anticorrelated functional networks. Proc Natl Acad Sci USA. 102(27): 9673–9678.
Fox MD, Zhang D, Snyder AZ, Raichle ME. 2009. The global signal and observed anticorrelated resting state brain networks. J Neurophysiol. 101(6):3270–3283.
Friston KJ, Holmes AP, Poline JB, Grasby PJ, Williams SC, Frackowiak RS, Turner R. 1995. Analysis of fMRI time-series revisited. Neuroimage. 2(1):45–53.
Frith CD, Frith U. 2006. The neural basis of mentalizing. Neuron. 50(4):531–534.
Gilbert SJ, Bird G, Frith CD, Burgess PW. 2012. Does "task difficulty" explain "task-induced deactivation?". Front Psychol. 3:125.
Gilbert SJ, Dumontheil I, Simons JS, Frith CD, Burgess PW. 2007. Comment on "wandering minds: the default network and stimulus-independent thought". Science. 317(5834):43. author reply 43.
Goldberg II, Harel M, Malach R. 2006. When the brain loses its self: prefrontal inactivation during sensorimotor processing. Neuron. 50(2):329–339.
Golland Y, Bentin S, Gelbard H, Benjamini Y, Heller R, Nir Y, Hasson U, Malach R. 2007. Extrinsic and intrinsic systems in the posterior cortex of the human brain revealed during natural sensory stimulation. Cereb Cortex. 17(4):766–777.
Gowen E, Poliakoff E. 2012. How does visuomotor priming differ for biological and non-biological stimuli? A review of the evidence. Psychol Res. 76(4):407–420.
Greicius MD, Flores BH, Menon V, Glover GH, Solvason HB, Kenna H, Reiss AL, Schatzberg AF. 2007. Resting-state functional connectivity in major depression: abnormally increased contributions from subgenual cingulate cortex and thalamus. Biol Psychiatry. 62(5): 429–437.
Greicius MD, Krasnow B, Reiss AL, Menon V. 2003. Functional connectivity in the resting brain: a network analysis of the default mode hypothesis. Proc Natl Acad Sci USA. 100(1):253–258.
Greicius MD, Menon V. 2004. Default-mode activity during a passive sensory task: uncoupled from deactivation but impacting activation. J Cogn Neurosci. 16(9):1484–1492.
Grossman E, Donnelly M, Price R, Pickens D, Morgan V, Neighbor G, Blake R. 2000. Brain areas involved in perception of biological motion. J Cogn Neurosci. 12(5):711–720.
Gusnard DA, Akbudak E, Shulman GL, Raichle ME. 2001. Medial prefrontal cortex and self-referential mental activity: relation to a default mode of brain function. Proc Natl Acad Sci USA. 98(7): 4259–4264.
Gusnard DA, Raichle ME. 2001. Searching for a baseline: functional imaging and the resting human brain. Nat Rev Neurosci. 2(10): 685–694.
Himberg J, Hyvarinen A, Esposito F. 2004. Validating the independent components of neuroimaging time series via clustering and visualization. Neuroimage. 22(3):1214–1222.
Ivry RB, Schlerf JE. 2008. Dedicated and intrinsic models of time perception. Trends Cogn Sci. 12(7):273–280.
Jastorff J, Orban GA. 2009. Human functional magnetic resonance imaging reveals separation and integration of shape and motion cues in biological motion processing. J Neurosci. 29(22): 7315–7329.
Josse J, Pagès J, Husson F. 2008. Testing the significance of the RV coefficient. Comput Stat Data Anal. 53(1):82–91.
Kandel S, Orliaguet JP, Viviani P. 2000. Perceptual anticipation in handwriting: the role of implicit motor competence. Percept Psychophys. 62(4):706–716.
Kelley WM, Macrae CN, Wyland CL, Caglar S, Inati S, Heatherton TF. 2002. Finding the self? An event-related fMRI study. J Cogn Neurosci. 14(5):785–794.
Knoblich G, Prinz W. 2001. Recognition of self-generated actions from kinematic displays of drawing. J Exp Psychol Hum Percept Perform. 27(2):456–465.
Lacquaniti F, Terzuolo C, Viviani P. 1983. The law relating the kinematic and figural aspects of drawing movements. Acta Psychol. 54(1–3):115–130.
Levit-Binnun N, Schechtman E, Flash T. 2006. On the similarities between the perception and production of elliptical trajectories. Exp Brain Res. 172(4):533–555.
Lloyd D. 2012. Neural correlates of temporality: default mode variability and temporal awareness. Conscious Cogn. 21(2):695–703.
Loula F, Prasad S, Harber K, Shiffrar M. 2005. Recognizing people from their movement. J Exp Psychol Hum Percept Perform. 31(1): 210–220.
Macar F, Anton JL, Bonnet M, Vidal F. 2004. Timing functions of the supplementary motor area: an event-related fMRI study. Brain Res Cogn Brain Res. 21(2):206–215.
Macar F, Vidal F, Casini L. 1999. The supplementary motor area in motor and sensory timing: evidence from slow brain potential changes. Exp Brain Res. 125(3):271–280.
Mantini D, Vanduffel W. 2013. Emerging roles of the brain's default network. Neuroscientist. 19(1):76–87.
Mars RB, Neubert FX, Noonan MP, Sallet J, Toni I, Rushworth MF. 2012. On the relationship between the "default mode network" and the "social brain". Front Hum Neurosci. 6:189.
McKiernan KA, Kaufman JN, Kucera-Thompson J, Binder JR. 2003. A parametric manipulation of factors affecting task-induced deactivation in functional neuroimaging. J Cogn Neurosci. 15(3): 394–408.
Merchant H, Harrington DL, Meck WH. 2013. Neural basis of the perception and estimation of time. Annu Rev Neurosci. 36(1):313–336.
Mitchell JP, Banaji MR, Macrae CN. 2005. The link between social cognition and self-referential thought in the medial prefrontal cortex. J Cogn Neurosci. 17(8):1306–1315.
Morillon B, Kell CA, Giraud A-L. 2009. Three stages and four neural systems in time estimation. J Neurosci. 29(47):14803–14811.

Mukamel R, Ekstrom AD, Kaplan J, Iacoboni M, Fried I. 2010. Single-neuron responses in humans during execution and observation of actions. Curr Biol. 20(8):750–756.
Nelissen K, Borra E, Gerbella M, Rozzi S, Luppino G, Vanduffel W, Rizzolatti G, Orban GA. 2011. Action observation circuits in the macaque monkey cortex. J Neurosci. 31(10):3743–3756.
Pavlova MA. 2012. Biological motion processing as a hallmark of social cognition. Cereb Cortex. 22(5):981–995.
Piaggi P, Menicucci D, Gentili C, Handjaras G, Gemignani A, Landi A. 2013. Adaptive filtering and random variables coefficient for analyzing functional magnetic resonance imaging data. Int J Neural Syst. 23(3):1350011.
Picard N, Strick PL. 2001. Imaging the premotor areas. Curr Opin Neurobiol. 11(6):663–672.
Pollick FE, Sapiro G. 1997. Constant affine velocity predicts the 1/3 power law of planar motion perception and generation. Vision Res. 37(3):347–353.
Preminger S, Harmelech T, Malach R. 2011. Stimulus-free thoughts induce differential activation in the human default network. Neuroimage. 54(2):1692–1702.
Qin P, Northoff G. 2011. How is our self related to midline regions and the default-mode network?. Neuroimage. 57(3):1221–1233.
Raichle ME, MacLeod AM, Snyder AZ, Powers WJ, Gusnard DA, Shulman GL. 2001. A default mode of brain function. Proc Natl Acad Sci USA. 98(2):676–682.
Rizzolatti G, Sinigaglia C. 2010. The functional role of the parieto-frontal mirror circuit: interpretations and misinterpretations. Nat Rev Neurosci. 11(4):264–274.
Robert P, Escoufier Y. 1976. A unifying tool for linear multivariate statistical methods: the RV-coefficient. J Royal Stat Soc C. 25(3): 257–265.
Rubinov M, Sporns O. 2010. Complex network measures of brain connectivity: uses and interpretations. Neuroimage. 52(3): 1059–1069.
Rubinov M, Sporns O. 2011. Weight-conserving characterization of complex functional brain networks. Neuroimage. 56(4):2068–2079.
Ruby P, Decety J. 2001. Effect of subjective perspective taking during simulation of action: a PET investigation of agency. Nat Neurosci. 4(5):546–550.
Saxe R, Powell LJ. 2006. It's the thought that counts: specific brain regions for one component of theory of mind. Psychol Sci. 17(8): 692–699.
Schneider F, Bermpohl F, Heinzel A, Rotte M, Walter M, Tempelmann C, Wiebking C, Dobrowolny H, Heinze HJ, Northoff G. 2008. The resting brain and our self: self-relatedness modulates resting state neural activity in cortical midline structures. Neuroscience. 157(1): 120–131.
Shinkareva SV, Gudkov V, Wang J. 2010. A network analysis approach to fMRI condition-specific functional connectivity. arXiv. 1008.0590.
Shinkareva SV, Mason RA, Malave VL, Wang W, Mitchell TM, Just MA. 2008. Using FMRI brain activation to identify cognitive states associated with perception of tools and dwellings. PLoS One. 3(1):e1394.
Spreng RN, Mar RA, Kim AS. 2009. The common neural basis of autobiographical memory, prospection, navigation, theory of mind, and the default mode: a quantitative meta-analysis. J Cogn Neurosci. 21(3):489–510.
Spreng RN, Stevens WD, Chamberlain JP, Gilmore AW, Schacter DL. 2010. Default network activity, coupled with the frontoparietal control network, supports goal-directed cognition. Neuroimage. 53(1):303–317.
Talairach J, Tournoux P. 1988. Co-Planar Stereotaxic Atlas of the Human Brain: 3-D Proportional System: An Approach to Cerebral Imaging (Thieme Classics). Stuttgart, Germany: Thieme.
Uddin LQ, Kelly AM, Biswal BB, Castellanos FX, Milham MP. 2009. Functional connectivity of default mode network components: correlation, anticorrelation, and causality. Hum Brain Mapp. 30(2):625–637.
van den Heuvel MP, Sporns O. 2011. Rich-club organization of the human connectome. J Neurosci. 31(44):15775–15786.
Viviani P, Flash T. 1995. Minimum-jerk, two-thirds power law, and isochrony: converging approaches to movement planning. J Exp Psychol Hum Percept Perform. 21(1):32–53.
Viviani P, Mounoud P. 1990. Perceptuomotor compatibility in pursuit tracking of two-dimensional movements. J Mot Behav. 22(3): 407–443.
Whitfield-Gabrieli S, Moran JM, Nieto-Castanon A, Triantafyllou C, Saxe R, Gabrieli JD. 2011. Associations and dissociations between default and self-reference networks in the human brain. Neuroimage. 55(1):225–232.